Proceedings of the 9th International Conference on Aluminium Alloys (2004)
Edited by J.F. Nie, A.J. Morton and B.C. Muddle



# Formation and Morphology of Hardening Nanostructures in an AlZnMg alloy

G.Riontino[1,2], A.Dupasquier[2,3], R.Ferragut[2,3,4], M.M.Iglesias[2,3], C.Macchi[4], M.Massazza[1,2], P.Mengucci[2,5], A.Somoza[4]

[1] Dipartimento di Chimica I.F.M., Università di Torino, Via P.Giuria 9, I-10125 Torino, Italy
[2] Istituto Nazionale per la Fisica della Materia (INFM), Italy
[3] Dipartimento di Fisica, Politecnico di Milano, Piazza L.da Vinci 32, I-20133 Milano, Italy
[4] IFIMAT, Universidad Nacional de Buenos Aires and CICPBA, Pinto 399, Tandil G7000BHG, Argentina
[5] Dipartimento di Fisica e Ingegneria dei Materiali e del Territorio, Università Politecnica delle Marche, Via Brecce Bianche, I-60131 Ancona, Italy

Keywords: AlZnMg alloys, thermal cycles, hardening nanostructures

## Abstract

Hardening of an AlZnMg alloy (similar in composition to the commercial AA7020) has been followed through different thermal treatments. The microstructure evolution has been analysed by a combination of techniques (DSC, PAS, SAXS and TEM).

## 1. Introduction

The mechanical properties of Al alloys of technological interest are determined by type, size and distribution of nanometric precipitates. Adequate knowledge of the elementary mechanisms controlling the structural evolution and the stability of alloys, in correlation with composition and thermal history, is at the basis of the modern metallurgy. This objective is actively pursued in many laboratories by combining spectroscopic techniques to classic bulk methods and direct imaging by electron microscopy and atom probe. In the present work, differential scanning calorimetry (DSC) and transmission electron microscopy (TEM) were applied, together with positron annihilation spectroscopy (PAS) and small angle X-rays scattering from synchrotron radiation (SAXS-SR), to investigate on the nanostructures formed in an AlZnMg alloy under the action of multistage heat treatments. Macroscopic aspects (mechanical properties and thermal stability) of the same subject have been recently studied [1]. In the present work, more attention is given to information on the morphology and to the chemistry of the precipitates, as it comes from TEM, PAS and SAXS-SR, in correlation with the conditions of nucleation and growth. Preliminary results were presented as a Conference paper [2]. New data are reported and discussed here, with account of the data given in Refs.[1-2].

## 2. Materials and Methods

In order to avoid precipitation effects due uncontrolled impurities, a laboratory alloy obtained by melting pure elements was used. On the other hand, the chosen composition (Al- 4.8 wt% Zn-1.3 wt% Mg) is basically the same of the commercial alloy AA7020, which is a typical high-strength alloy for the transport industry. After casting, the material was homogenised in air at 465°C for 12 hours.

The samples, prepared in due form and size for the different experimental techniques, were water quenched after 1 hour at 465°C and then thermally treated in various ways, as specified in the next Section. Disc shaped samples, about 50 mg in weight, were used for DSC measurements in a TA 2010 apparatus (scanning rate 20 K/min). PAS was applied in two variants, namely PALS (positron annihilation lifetime spectroscopy) and CDB (coincidence Doppler broadening). The PALS set-up was adjusted on privileging counting rate (~1300 counts/s) against resolution (250 FWHM); one-component analysis was adopted. CDB spectra were taken with a statistics of at least $5x10^7$ counts, using two Ge spectrometers (individual resolution ~1.2 keV at 0.511 MeV) (for an introduction to PAS, see [3]). SAXS experiments were performed at ESRF (beamline BM26B). The Guinier radius $R_G$ of the scattering centres and the integrated intensity $Q_0$ were obtained from standard analysis of SAXS-SR data [4]. TEM observations were performed by a Philips CM200 microscope at 200 kV.

## 3. Results and Discussion

The starting point of the present work is Ref. [1]. The main results of [1] can be summarised as follows. Several heat treatments were tested (see [1] for the motivations of the choice). The highest microhardness attained by application of these treatments is reported in Table 1, together with the corresponding thermal history.

Table 1: Microhardness attained by different heat treatments. Values marked by an asterisk were obtained after interrupting the treatment before reaching a saturation or the peak ageing value. The average experimental uncertainty is of the order of ±3 VHN. After Riontino and Massazza [1].

| Temper | Solution treatment | 1st stage | 2nd stage | 3rd stage | Microhardness (VHN) |
|---|---|---|---|---|---|
| **A** | as-quenched | | | | 43 |
| **B** | as above | 42 days/ RT | | | 104* |
| **C** | as above | 30 min /150°C | 17 days/ RT | | 97* |
| **D** | as above | 4 days/RT | 7 days /95°C | | 135* |
| **E** | as above | 4 days/RT | 8 hours/95°C | 8 hours/150°C | 130 |
| **F** | as above | 4 days/RT | 2 days/150°C | | 112 |
| **G** | as above | 30 min/150°C | 100 hours/ RT | 1 day/150°C | 109 |
| **H** | as above | 21 days /150°C | | | 55 |

The DSC traces depicted in Figure 1 show the following sequence of endothermic (dissolution) and exothermic (formation) stages:

- 100-190°C: endothermic stage *d1*, attributed to dissolution of small solute clusters in the as-quenched material and of GP(I) zones formed during RT ageing. This stage is very well developed with tempers B and C; it becomes weaker after exposure at 95°C (D) and disappears after heating at 150°C (E, F, G, H).
- 200-270°C: endothermic stage *d2*, attributed to the dissolution of vacancy-rich clusters (A, B, C) or of GP(II) zones (D, E) and η' precipitates (F, G). It cannot be isolated after the H temper.
- 250-300°C: exothermic peak *p*, attributed to precipitation of η particles occurring during the DSC experiment. Well developed after tempers A, B, C, D, E; weak or invisible after tempers that imply extended exposure to 150°C (tempers F to H).
- 300-360°C: endothermic stage *d*, attributed to dissolution of η particles formed either during the DSC scan (tempers A to E) or during extended exposure to 150°C (tempers F to H).

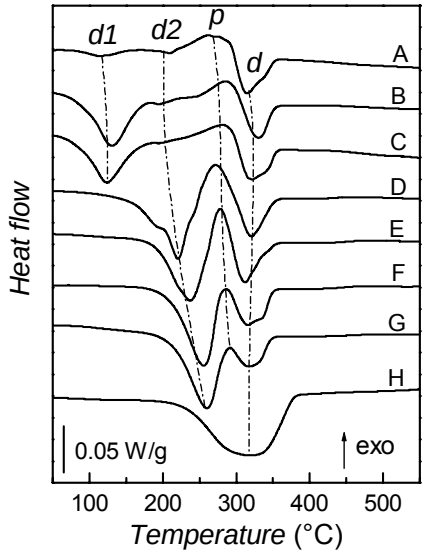


Figure 1: Calorimetric traces taken at 20K/min. Curve labels corresponding to the tempers reported in Table 1. After Riontino and Massazza [1].

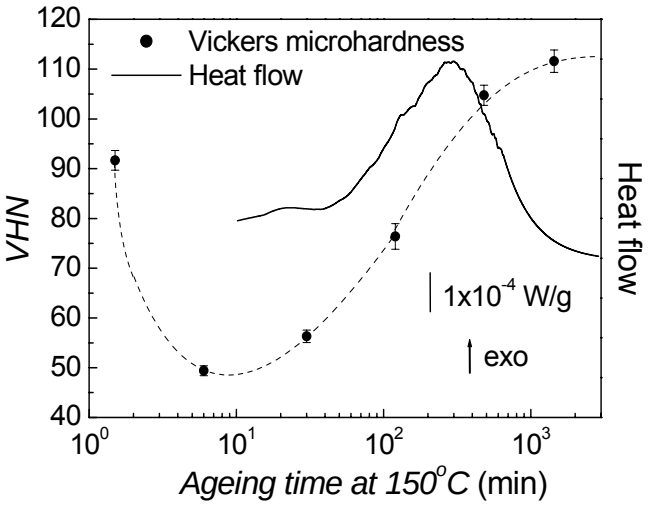


Figure 2: Heat flow and Vickers microhardness evolution during isothermal ageing at 150°C after 4 days at RT.

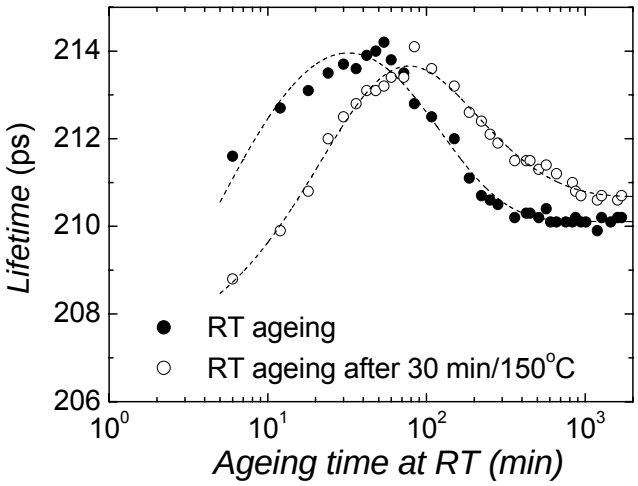


Figure 3: Positron lifetime evolution at RT for treatments B (filled circles) and C (open circles).

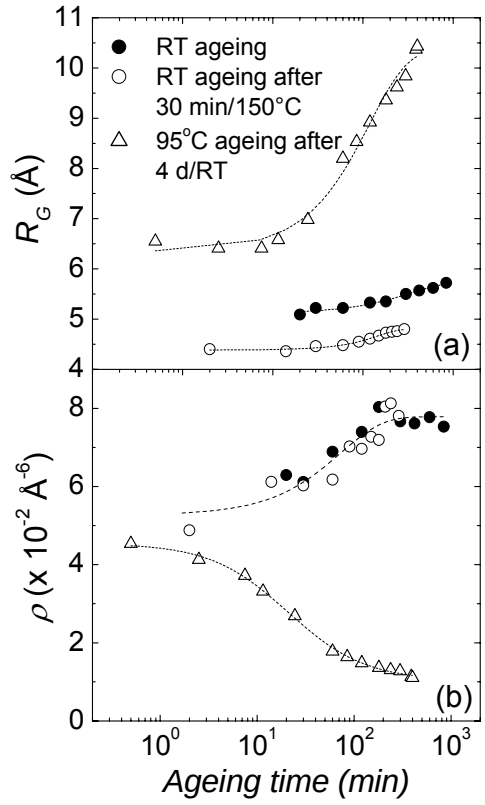


Figure 4: Evolution of the Guinier radius (panel a) and of the ratio ρ (panel b) for aggregates formed during treatments B (filled circles), C (open circles) and D (triangles).

The above interpretation of DSC curves is consistent with isothermal calorimetric measurements, showing the presence of exothermic stages corresponding to the precipitation of hardening phases. Figure 2 reports, as an example, the evolution at 150°C whose final stage corresponds to temper F. During the first minutes of ageing the hardness decreases due to the dissolution of small GP zones formed in the course of natural ageing at RT [5]; later, after about 10 min, the hardness increases in coincidence with the formation of semicoherent η' precipitates (exothermic peak in the figure).

Tempers B and C give very similar results: no substantial diversity is observed in the calorimetric traces shown in Figure 1, and the small difference in the microhardness values reported in Table 1 can be reasonably ascribed to the different duration of the RT ageing stage. The similarity of bulk properties reflects a corresponding similarity at the nanostructural level, as observed by PALS and SAXS-SR. The evolution of the positron lifetime (see Figure 3), which reflects variations of the chemical composition in contact with vacancies, suggests that the solute content of the GP(I) zones formed after extended RT ageing is not much affected by previous short heating at 150°C. GP(I) zones are smaller for the C than for the B temper; however, the difference in the Guinier radius $R_G$ is no more than 10% (see Figure 4a). SAXS-SR results also indicate that the number of X rays scattering centres $\nu$ is similar in the two cases. This statement is supported by the data shown in Figure 4b, depicting the evolution of $\rho = Q_0 / R_G^3$; this ratio is approximately proportional to $\nu$ (proportionality would be exact for small volume fraction and constant chemical composition of the precipitates). It is also interesting that $\rho$ tends to saturate above 200 min; after this time, further aggregation of solute seems to produce growth rather than new nucleation of GP(I) zones.

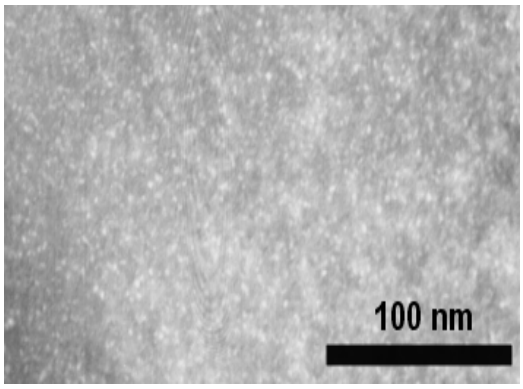


Figure 5: TEM dark field image taken after 4 days at RT and 8 hours at 95°C (orientation $[112]_{Al}$).

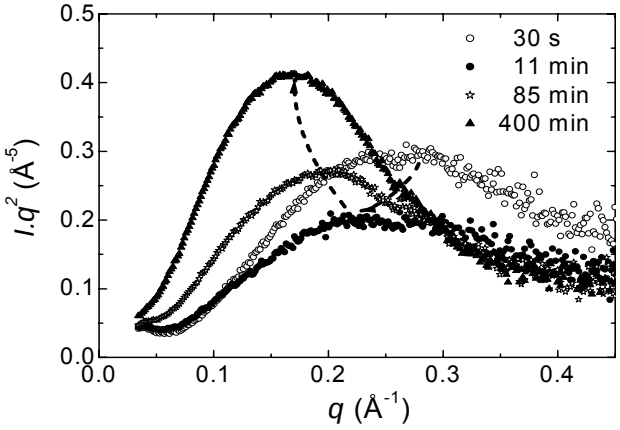


Figure 6: SAXS-SR distributions for various ageing times at 95°C after 4 days at RT.

Treatments including an extended stage at 95°C (D and E) give the strongest hardening effect. DSC results suggest associating the hardness increase to the enhancement of the *d2* endothermic stage. Identification of the corresponding structure with GP(II) zones is consistent with TEM images (Figure 5) of small spherical precipitates (about 2 nm in diameter). The size evaluation from TEM is in agreement with SAXS-SR results shown in Figure 4a (triangles); the data of Figure 4b also suggest a decreasing trend of the number of X rays scattering centres that would imply growth by coalescence. SAXS-SR $Iq^2$ distributions, showing the effects of precipitate growth, are reported in Figure 6 for various ageing times. During the first minutes of ageing small aggregates are dissolved and are gradually replaced in the course of the ageing by medium sized GP(II) zones. The zones grown at 95°C are remarkably stable: the only evident difference in DSC traces for tempers D and E, which is brought in by additional heating at 150°C for 8 hours, is the complete suppression of the *d1* stage (residual GP(I) zones after heating at 95°C) and a slight displacement toward higher stability of the *d2* stage.

However, the CDB results*, reported in Figure 7, suggest that the important effect of additional heating at 150°C is the transformation of coherent GP(II) zones into semicoherent η' particles. The key to immediate (qualitative) reading of the curves of Figure 7 is to keep in mind that the large bumps appearing at momentum values $|p_x| > 2$ atomic units are due to positron encounters with fast Zn electrons; the height of the bumps is approximately proportional to the Zn atomic concentration near to the annihilation site (40 at. % Zn would approximately correspond to the thin solid line, which is a reference curve taken for cold-rolled Zn and scaled down by a factor 0.4 for the convenience of representation). In the lower panel of Figure 7 the curves are for ageing at 95°C after 4 days at RT (temper D): the data show that this treatment has almost no effect on the Zn concentration seen by positrons. On the contrary, the curves reported in the upper panel, which refer to ageing at 150°C after 4 days at RT + 8 hours at 95°C (temper E) display a remarkable weakening of the Zn signature. This effect cannot be reasonably

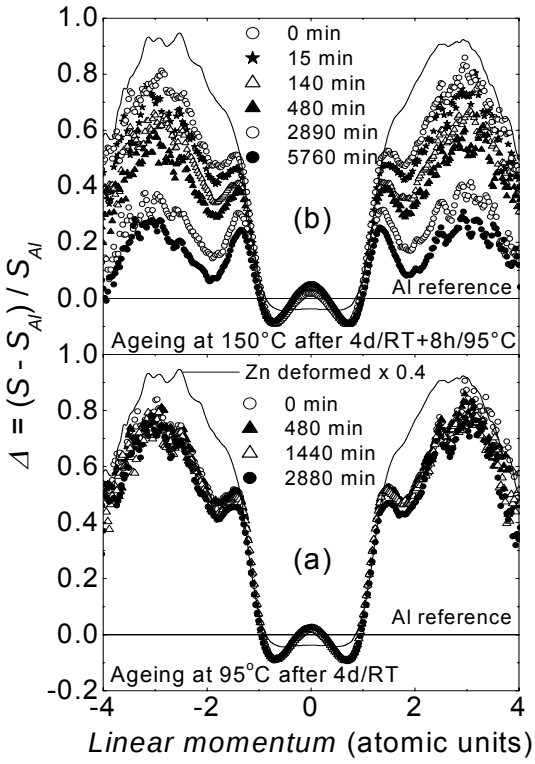


Figure 7: CDB curves. Panel (a): 4 days at RT + various times at 95°C; panel (b): 4 days at RT + 8 hours at 95°C (▲of panel a)+ various times at 150°.

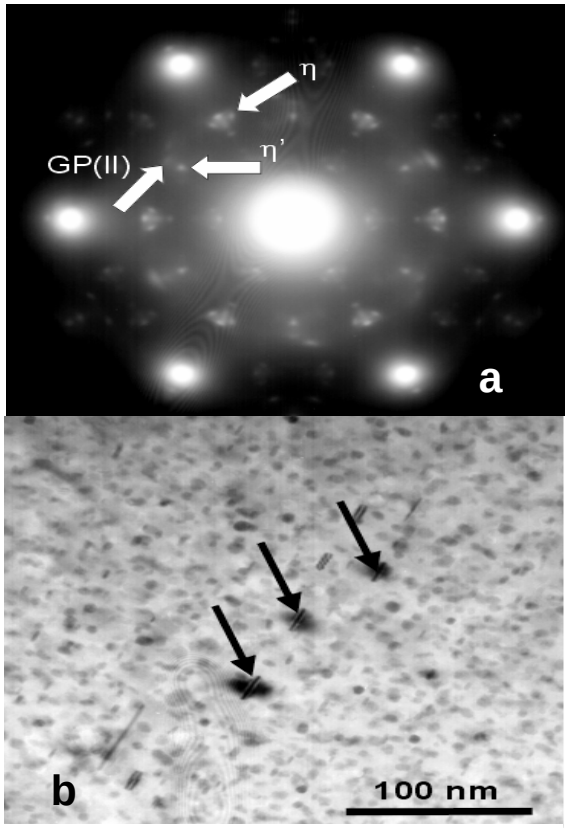


Figure 8: TEM results after 4 days at RT + 12 hours at 150°C: (a) diffraction pattern, $[111]_{Al}$; (b) bright field image, $[112]_{Al}$

attributed to a reduction of the Zn content of the precipitates; most probably, it comes from a reduction of positron trapping at vacancies inside Zn-rich precipitates due to competitive trapping at the misfit interfaces between η' particles and the matrix.

According to Table 1, heating at 150°C is always less beneficial for strengthening than heating at 95°C; however the difference between treatment H, which is a typical T6 temper, and multi-stage treatments E, F and G, is substantial. From the microscopic point

* The CDB curves shown in Figure 7 represent the relative difference $\Delta = (S - S_{Al})/S_{Al}$ between the energy spectrum *S* of the positron annihilation radiation taken for the alloy and a reference spectrum $S_{Al}$ (pure Al in the present case), plotted against the component along the detection direction of the linear momentum of the annihilated electron-positron pair [6].

of view, this difference corresponds to different species and sizes of precipitates. TEM diffraction patterns taken after solution treatment + 30 hours at 150°C have shown that direct heating of the supersaturated solid solution produces mainly η particles, with a less important presence of GP(II) zones and η' particles. The corresponding TEM images show a distribution of precipitates with sizes from 5 to 15 nm. On the contrary, in the other cases the η' phase is dominant, and the precipitate sizes are finer. TEM results are reported in Figure 8 for a sample aged 4 days at RT + 12 hours at 150°C; the image shows spheroidal precipitates from 4 to 8 nm in diameter, with occasional elongated needle-like particles (arrows); the two species of precipitates are often associated. As mentioned above, the CDB data of Figure 7 encourage to explain the preferential formation of η' particles after a previous treatment at 95°C (temper E) by the transformation GP(II)→η' occurring after a further size increase, but without affecting the dispersion of the precipitates. Discussing the mechanism that leads to preferential formation of a well dispersed η' phase in tempers F and G needs more guessing. The effects of these two tempers on DSC traces and on ultimate hardness are very similar; as in the case of tempers B and C, 30 min heating at 150°C prior to RT ageing turns out to be substantially irrelevant. Thus, it can be safely assumed that, in both cases, at the beginning of the last heating stage the material contains a well-developed population of GP(I) zones. However, the transformation GP(I)→η' is highly unlikely, as GP(I) are rapidly dissolved when the temperature is raised to 150°C. Therefore, one is lead to suspect that during the RT dwell time other solute aggregates, more stable than GP(I), develop from Zn-vacancy-rich clusters already present after quenching. Close comparison of curves B and C with A in Figure 1 indeed shows that a broad dissolution stage might be present in B and C between about 200 and 260°C after RT ageing. This stage would be the signature of the small precipitates forming nucleation seeds for further aggregation of solute at higher temperature, eventually leading to precipitation of the η' phase.

## 4. Conclusions

The conclusions of the present work can be summarised as follows.

- RT ageing gives dominant formation of GP(I) zones (about 1 nm in diameter). Coalescence begins after about 200 min. Strong variations of the positron lifetimes indicate that the average chemical composition of the precipitates changes during ageing. Hardening continues without apparent saturation within the duration of the experiment.
- Heating for 30 min at 150°C prior to RT ageing does not give other measurable effect on the precipitates than a 10 % reduction in diameter.
- Heating at 95°C gives the strongest hardening effect, with no saturation within the duration of the experiment (135 VHN after 4 days at RT + 7 days at 95°C). The size of the precipitates is about 2 nm at the end of the experiment. Consistent evidence from CDB and TEM supports the identification of the dominant precipitates with coherent GP(II) zones.
- T6 temper at 150°C is not effective for hardening. The size of the precipitates increases up to about 15 nm in diameter. The dominant phase is η.
- Ageing at RT and at 95°C prior to heating at 150°C favours the formation of smaller precipitates (up to 8 nm in diameter). The dominant phase is η'. CDB results support the formation of misfit interfaces between matrix and precipitates.
- The transformation GP(II)→η' is suggested to be the mechanism by which pre-ageing at RT or at 95°C affects the subsequent ageing at 150°C. However, the evidence for this interpretation is stronger when preageing is carried out at 95°C than at RT.

## Acknowledgments

This work has been performed under the Project FIRB RBAU0RW84 (Ministero Istruzione Università e Ricerca, Italy), and the Project N°9F, 2002-2003 (Ministero Affari Esteri, Italy, and Secreterìa de Ciencia, Tecnologìa y Producciòn, Argentina).

## References

[1] G. Riontino and M. Massazza, Phil. Mag. (in press).
[2] A. Dupasquier, R. Ferragut, M. M. Iglesias, C. E. Macchi, M. Massazza, P. Mengucci, G. Riontino and A. Somoza, Mater. Sci. Forum, 445-446, 16-20, 2004.
[3] A. Somoza and A. Dupasquier, J. Mater. Processing Technology 135**,** 83-90, 2003.
[4] O. Glatter and O. Kratky, Small Angle X-ray Scattering, Academic Press Inc., London, 1982.
[5] R. Ferragut, A. Somoza and A. Dupasquier, J. Phys. Cond. Matter 10, 3903-3918, 1998.
[6] A. Somoza, M. P. Petkov, K. G. Lynn and A. Dupasquier, Phys. Rev. B 65, 094107, 2002.